Chemical Physics 139 (1989) 201–220
North-Holland

WAVEPACKET DANCING: ACHIEVING CHEMICAL SELECTIVITY BY SHAPING LIGHT PULSES

R. KOSLOFF
Department of Physical Chemistry and the Fritz Haber Research Center for Molecular Dynamics, The Hebrew University, Jerusalem 91904, Israel

S.A. RICE, P. GASPARD, S. TERSIGNI
Department of Chemistry and The James Franck Institute, The University of Chicago, Chicago, IL 60637, USA

and

D.J. TANNOR
Department of Chemistry, Illinois Institute of Technology, Chicago, IL 60637, USA

Received 28 June 1989

The Tannor–Rice pump–dump scheme for controlling the selectivity of product formation in a chemical reaction is improved by development of a method for optimizing the field of a particular product with respect to the shapes of the pump and dump pulses. Numerical studies of the optimization of product yield in a model system of the same type as studied by Tannor and Rice illustrate the enhancement possible with pulse shaping.

1. Introduction

The use of light to induce reactions is as old as chemistry. The traditional light source – at first the sun and later diverse laboratory lamps – emit incoherent polychromatic or incoherent line radiation which is, by modern standards, of low intensity. Conventional practice in photochemistry [1] uses the (linear) absorption of incoherent radiation to prepare an initial excited state which is allowed to evolve under the molecular Hamiltonian. Although the prepared initial state can have the energy necessary to overcome the barriers to several possible reactions, in practise there is no better control of selectivity of the products formed in these reactions when photochemical excitation is used than with any other incoherent excitation that prepares the same initial state.

The opportunity to remove the restrictions of conventional practice in the use of light to aid chemical synthesis has been provided by the many developments in laser technology in the last twenty years. In particular, laser radiation is (or can be) monochromatic, coherent and very intense. The possibility that the unique characteristics of laser radiation can be exploited to improve the selectivity of product formation in a chemical reaction has stimulated the proposal and testing of many schemes [2]. These schemes can be crudely grouped according to the particular characteristic of the laser radiation that is exploited, i.e. monochromaticity, intensity and coherence.

To date the successful schemes are all associated with utilization of the monochromaticity of the laser radiation to selectively generate reaction of one component of a mixture, e.g., isotope separation by differential excitation and subsequent reaction of one component of a mixture whose species differ only in isotopic composition. In contrast, attempts to use the monochromaticity of laser radiation to select a particular intermediate state of a molecule, with the hope that subsequent evolution of said state would lead to reaction with preferential

0301-0104/89/$ 03.50
(North-Holland)

formation of a desired product, have not had much success. Although it is, in principle, possible to excite an unusual very long lived molecular resonance which is dominantly coupled to a particular exit channel, and thereby control product selectivity, very few such cases are known. One case worth citing, because of the thoroughness of the investigation, is the fragmentation of D_2H^+ to form $H^+ + D_2$ or $D^+ + DH$ [3,4]; in this case near degenerate long lived resonances yield, on excitation, preferentially one or the other of the cited products.

Similarly, attempts to use the very high intensity of laser radiation to influence the selectivity of product formation in a reaction, say, by multiphoton excitation of a potentially reactive chromophore group in a molecule, have not been generally successful.

In view of the analysis and results presented later in this paper, it is worthwhile noting that methods for controlling the selectivity of product formation in a chemical reaction which are based on only the monochromaticity and/or the intensity of the exciting radiation are fundamentally passive, in the sense that after preparation of the initial excited state the entire course of the temporal evolution is governed by the molecular Hamiltonian. Such methods suffer from the competition between intramolecular redistribution of energy and reaction; since the rate of the former is usually much larger than the rate of the latter the memory of the character of the initial state is erased to an extent sufficient to reduce or completely eliminate control of product selectivity based on initial state preparation.

The most recent work on control of product formation in a chemical reaction focuses on active methods, i.e. those in which the evolution of the prepared state is partially controlled by the free molecule Hamiltonian and partially controlled by external means. Brumer and Shapiro [5] have shown that selectivity of product formation can be induced by tuning the phase difference between two cw laser sources working at different frequencies; this scheme exploits the coherence properties of the radiation in the frequency domain. Tannor and Rice [6] and Tannor, Kosloff and Rice [7,8] have shown that selectivity of product formation can be induced by shaping and spacing pump and dump laser pulses. In the limiting case that the electromagnetic fields associated with the pulses are small enough that perturbation theory can be used to describe the evolution of the molecule–field system, Tannor and Rice showed that their scheme could be formulated as a variational problem [6], where the dump pulse shape (thought of as also including pulse separation as in a multipeaked function) is the function to be determined given the form of the system Hamiltonian and the criterion defining the final state desired. This variational formulation of the calculation of the dump pulse shape is equivalent, with the constraints used, to an optimal control theory calculation with the dump pulse shape as the control function. In the perturbation theory limit that control problem can be solved analytically using the calculus of variations. In the limit when the electromagnetic fields associated with the pulses are large enough that the system must be described as consisting of mixed field–matter states Tannor, Kosloff and Rice [7] maximized the selectivity of product yield approximately by controlling the time delay between the pump and dump pulses, without allowing for variation of the shapes of the pulses. The possibilities inherent in the full formalism of optimal control theory without resort to the perturbation theory limit and without imposing constraints on the pulse shapes, when applied to enhancement of selectivity of product formation in a chemical reaction, have been explored by Rabitz and co-workers [9]. The practical application of their ideas has, to date, been limited to the study of linear chains of harmonic oscillators. The work presented in this paper is an extension of the work of Tannor and Rice and has features in common with the optimal control theory approach of Peirce, Dahleh and Rabitz.

Briefly put, the Tannor–Rice scheme utilizes an excited electronic state to mediate reaction on the ground electronic state potential energy surface. Consider a ground state potential energy surface which has (a) a stable equilibrium geometry and (b) at least two channels which, asymptotically, correspond to different products. Further, assume that the system has an excited state whose potential energy surface has, in general, a displaced equilibrium configuration and rotated coordinates. A (first) laser pulse transfers amplitude from the ground to the excited state potential energy surface. Because the wavepacket formed on the excited state surface is not an eigenfunction of the Hamiltonian for that surface, it evolves spatially and temporally. At the right moment a second laser pulse transfers some of the amplitude back to the ground state surface in such a way that amplitude preferentially emerges, eventually, in a particular reactive channel. The problem to be solved is the determination of the sequence of light pulses that optimizes the desired product selectivity. It is worthwhile noting that this scheme is symmetric with respect to the roles of the several potential energy surfaces; although it would require an extra step to start the system in an excited state, selectivity of reaction on an excited state surface can be modulated by flow of amplitude on the ground state surface [6], inverting the roles of excited and ground state surfaces described above.

Tannor and Rice developed a practical scheme to enhance the selectivity of product formation in the limiting case of very short pump and dump pulses. The advantage of focusing attention on the very short pulse limit is that the classical–quantum mechanical correspondence between a trajectory and wavepacket motion can be used to develop a physical picture of the system and its evolution. In the Tannor–Rice scheme a vertical transition from the ground state surface to the excited state surface defines the initial state of the wavepacket on the excited state surface. The evolution of the wavepacket on the excited state surface is then followed. At selected times a vertical transition is induced, transferring some amplitude back to the ground state surface, and the evolution on the ground state surface is then followed until a product (or, possibly, no product) is formed. This procedure maps the time delay between pump and dump pulses with respect to selectivity of product formation, e.g., the ratio of numbers of molecules of products formed. Note that in the simplest version of this procedure the pump and dump pulse shapes are fixed and, although the wavepacket shape and width changes as it evolves on the potential energy surface, only the time interval between pump and dump pulses is used to modify the product selectivity. It is very convenient that in the very short pulse limit it is found that the ensemble of classical trajectories of a Wigner swarm representing the wavepacket accurately mimics the quantum mechanical flow of amplitude [7], thereby permitting a simple picture of the selectivity method to be developed and, also, permitting the use of classical mechanical simulations for a first approximation to the construction of the selectivity mapping referred to above.

The application of the scheme just described to real experiments raises two serious problems. First, the light pulses used to transfer amplitude between the ground and excited state surfaces necessarily have nonnegligible duration on the time scale of the molecule vibrations, causing the transfered amplitude to be more spatially extended than would occur in the limiting case of delta function pulses. Second, the anharmonic components of the potential energy functions of the two surfaces will generate a spreading of the initially compact wavepacket. Both of these effects act to decrease the selectivity of product formation and, possibly, could eliminate any selectivity for realistic pump–dump conditions for a particular molecule. Finally, when the effects mentioned are important, the semiclassical scheme used by Tannor and Rice to predict which time delays should be explored by full quantum mechanical calculations breaks down. Of course, the full quantum mechanical description of the evolution of the coupled field–molecule states remains valid under all conditions, but the simple picture in which the enhancement process is generated by a favorably timed transfer of amplitude from the mediating excited state potential energy surface to the ground state surface on which the reaction occurs, is lost when the semiclassical description is invalid.

The spatial extension and degradation of the wavepacket mentioned above are consequences of the interference between components of the wavepacket, which interference changes as the wavepacket evolves under the influence of the external field and the molecular Hamiltonian. This observation suggests that it is, in principle, possible to use the external field to partially reconstruct (refocus) the wavepacket [7]. In fact, one can imagine a selectivity of product formation scheme in which interference effects are utilized to enhance formation of the desired product. Specifically, one can imagine using the coherence properties of the light to produce constructive interference of the wavepacket in the desired exit channel. In the remainder of this paper just such a scheme is described.

It is important to understand the sense in which we use the word "optimize". As will be readily seen from the analysis presented, to the extent that constraints are used to reduce the dimensionality of the control parameter space, the resulting controlled optimization might better be called "enhancement". To be specific, the original Tannor–Rice pump–dump pulse scheme [6] allowed for variation of pulse shapes and pulse separation in the maximization of the yield of a particular product, but the strong field implementation reported by Tannor, Kosloff and Rice [7] was carried out for fixed pump and dump pulse shapes, using only the pulse separation to alter the phase relationships between the pump and dump pulses. During the interval when the wavepacket propagates freely on the excited state potential energy surface its evolution is governed by the free molecule Hamiltonian. Tannor, Kosloff and Rice show that for some potential energy surfaces this "free" propagation leads to wavepacket spread that destroys the selectivity of product formation, whereas for other potential energy surfaces selectivity is maintained despite the induced wavepacket spreading. Tannor, Kosloff and Rice also show that application of a steady field to the molecule while the wavepacket is on the excited state potential energy surface can alter the evolution of the wavepacket. In principle, then, within the framework of the scheme proposed, greater control over the selectivity of product formation can be generated by modifying the wavepacket evolution between pump and dump pulses than by allowing free evolution between pump and dump pulses, and even greater control over the selectivity of product formation can be generated by also shaping the pump and dump pulses. The local optimization scheme considered in this paper removes some of the superficially clearcut distinctions between the pump and dump pulses and any field acting during the wavepacket propagation period; the global optimization scheme makes no distinction between pump and dump pulses, defining instead one complex pulse that induces (multiply) both processes. By choosing the electromagnetic field waveform in the fashion described below the pulse shapes become complex, possibly multipeaked. The action of the shaping field has, for the purpose of controlling the evolution of the excited molecule, some but not all of the characteristics of the separately optimized pump pulse, intermediate field and dump pulse described above. Of course, whatever the optimization scheme, whether "complete" or incomplete, the molecular dynamics is controllable only to the extent that the combined molecule–electromagnetic field Hamiltonian permits.

2. The selectivity scheme and its optimization

2.1. General remarks

The chemical model which was chosen for this calculation is the same as that used to test the fixed Gaussian pulse-variable time delay scheme [7]. This model is defined by two potential energy surfaces; the ground state surface has two exit channels corresponding to the rearrangement reaction

$$\begin{aligned} \mathrm{AAB} &\to \mathrm{AA+B}, \quad \text{channel A} \\ &\to \mathrm{A+AB}, \quad \text{channel B}\,. \end{aligned}$$

The ground state potential energy surface used is identical to the one used in the previous papers [6–8]. The excited state potential energy surface is, as already mentioned, used to mediate the reaction on the ground state surface. In order to magnify the effects of delocalization of the wavepacket on the excited state surface, an extremely anharmonic potential function was chosen, but with the same functional form as for the ground state. The parameters of the two potential energy surfaces, and the dimensions of the grid used for propagation of the amplitude on these surfaces, are listed in table 1. Fig. 1 displays a stereoscopic view of the two potential energy surfaces.

The equation of motion of the coupled amplitudes on the two potential energy surfaces can be written

$$\mathrm{i}\frac{\partial}{\partial t}\begin{pmatrix}\psi_{\mathrm{u}}\\ \psi_{\mathrm{g}}\end{pmatrix}=\begin{pmatrix}\mathbf{H}_{\mathrm{u}} & \mathbf{V}_{\mathrm{gu}}\\ \mathbf{V}_{\mathrm{ug}} & \mathbf{H}_{\mathrm{g}}\end{pmatrix}\begin{pmatrix}\psi_{\mathrm{u}}\\ \psi_{\mathrm{g}}\end{pmatrix}, \tag{2.1}$$

where ψ_{u} is the projection of the wavefunction on the upper surface, ψ_{g} is the projection of the wavefunction on the ground state surface, and $\mathbf{H}_i$ is the upper/lower surface Hamiltonian. Of course $\mathbf{H}=\mathbf{T}_i+\mathbf{V}_i$ where $\mathbf{T}_i=p^2/2m$ is the kinetic energy operator, $\mathbf{V}_i$ is the upper/lower surface potential energy, $\mathbf{V}_{\mathrm{ug}}$ is the interaction poten-

Table 1
Parameters of potential, grid and time step

$$V(l,\theta)=D(\theta)(1-\exp\{\beta(\theta)[l-l_{\mathrm{eq}}(\theta)]\})^2+V_0,\quad D(\theta)=D_0-D_1H_2(\theta)\exp[-(\theta-\pi/4)^2/2\sigma_D^2],$$
$$\beta(\theta)=\beta_0-\beta_1\exp[-(\theta-\pi/4)^2/2\sigma_\beta^2],\quad l_{\mathrm{eq}}(\theta)=l_0+l_1\exp[-(\theta-\pi/4)^2/2\sigma_l^2],\quad H_2(\theta)=4(\theta-\pi/2)^2/\sigma_D^2-2$$

Potential parameters

surface	D_0	D_1	σ_D^2	β_0	β_1	σ_β^2	l_0	l_1	σ_l^2	V_0
ground	0.1705	0.01912	0.007615	1.0584	0.3334	0.04386	8.045	2.823	0.0685	0
excited	0.1705	0.01912	0.1	1.0584	0.3334	0.04386	7.635	2.823	0.0685	0.07

Grid parameters

grid spacing	$\Delta x=0.1$ au	$\Delta y=0.1$ au
	$N_x=64$	$N_y=64$
or	$N_x=96$	$N_y=96$
mass scaling	$R_1=-l\cos\theta+10$	$R_2=-l\sin\theta+10$
	$x=\sqrt{2}R_1$	$y=R_2+\frac{1}{2}R_1$

Time propagation

propagation time step	SOD	$\Delta t=0.5$ au	$t_f=3400$ au					
	P5	$\Delta t=2.0$ au	$t_f=2000$ au					
pulse parameters	$\omega_1=0.0915$	$\omega_2=0.073$	$\sigma_1=0.95$	$\sigma_2=0.95$	$A_1=0.022$	$A_2=0.022$	$t_1=320$	$t_2=1640$

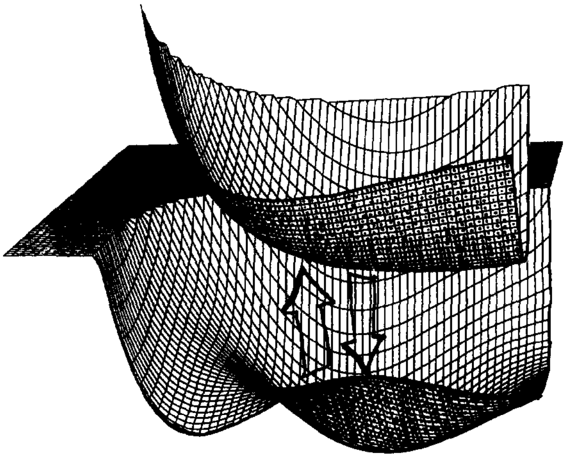

Fig. 1. Stereoscopic view of the ground and excited state potential energy surfaces. The arrows show, schematically, the amplitude transfers associated with the pump and dump pulses.

tial which we take to have the form $\mathbf{V}_{\mathrm{ug}}=\mu_{\mathrm{ug}}\mathcal{E}(t)$, $\mathbf{V}_{\mathrm{gu}}=\mu_{\mathrm{gu}}\mathcal{E}^*(t)$, where μ_{ug} is the dipole operator and $\mathcal{E}(t)$ represents the amplitude of a semiclassical electromagnetic field.

2.2. Pulse optimization

The main question to be addressed now is the following: how does one choose the correct form for the light pulse $\mathcal{E}(t)$ which leads to a particular chemical outcome? The problem is one of inversion: given the final wavefunction one has to determine the electromagnetic field waveform $\mathcal{E}(t)$. Although a general approach to solving this inversion problem has been suggested, based on use of an integral equation [6,9], solution of the integral equation for realistic systems is very difficult and is beyond the scope of the present work. The Gaussian pulse approach described previously [7] can be regarded as an inversion algorithm: $\mathscr{E}(t)$ is obtained as a series of delta functions in time, where the time delay optimizes the chemical selectivity.

It is convenient to introduce the elements of our pulse optimization scheme in two stages, which also happens to follow how our own understanding developed. In the first stage of the analysis we introduce an intuitively based iteration procedure for optimization of the pulse shapes. This procedure leads to a "local", or instantaneous, optimal prescription for transferring amplitude from surface to surface. As implied by the word "instantaneous", this procedure is local with respect to time. In the second stage of analysis we use optimal control theory to derive a global optimization procedure for determination of the pulse shapes; the term "global" implies that the target function is optimized over the duration of the evolution of the wavepacket–external field combination. All the key elements of the global optimization procedure are to be found in the first developed intuitive optimization procedure.

In section 3 we report the results of calculations using both the local and the global optimization of pulse shape procedures. There it is demonstrated that both procedures converge and, indeed, define a scheme for enhancement of amplitude in the desired product channel. Although the global optimization procedure will always give a better answer than the intuitive local optimization procedure, the latter appears to be a convenient algorithm for generation of a good initial guess for the former.

2.2.1. Local optimization scheme

The central idea in this work is to use the propagation equation (2.1) for the determination of the electromagnetic field waveform $\mathscr{E}(t)$. The problem is analogous to that of tying together two strings starting from two ends: at $t=0$ where the wavefunction amplitude is all on the ground state surface and at $t=t_f$ when the wavefunction amplitude is to be found in the desired exit channel, also on the ground state surface. The meeting point

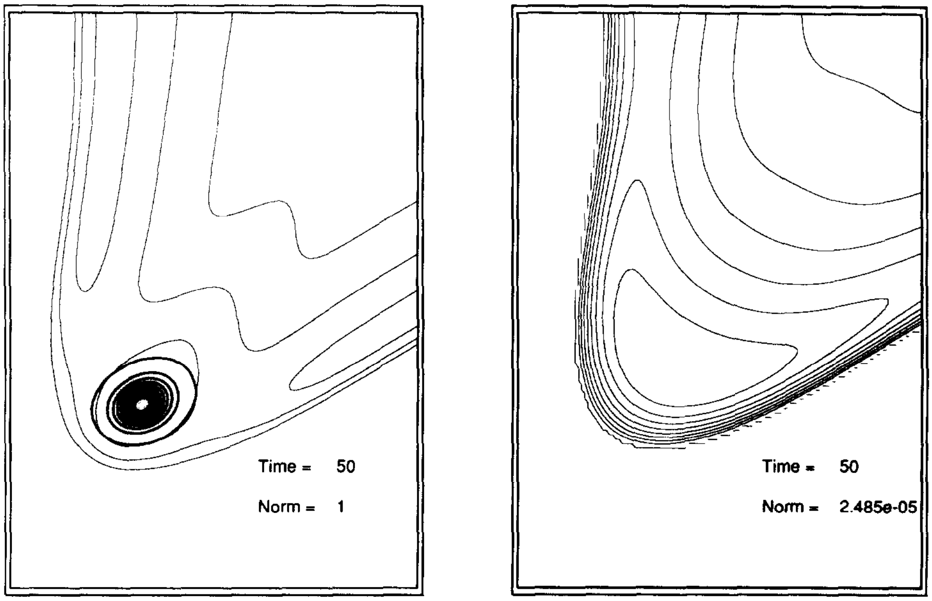

a

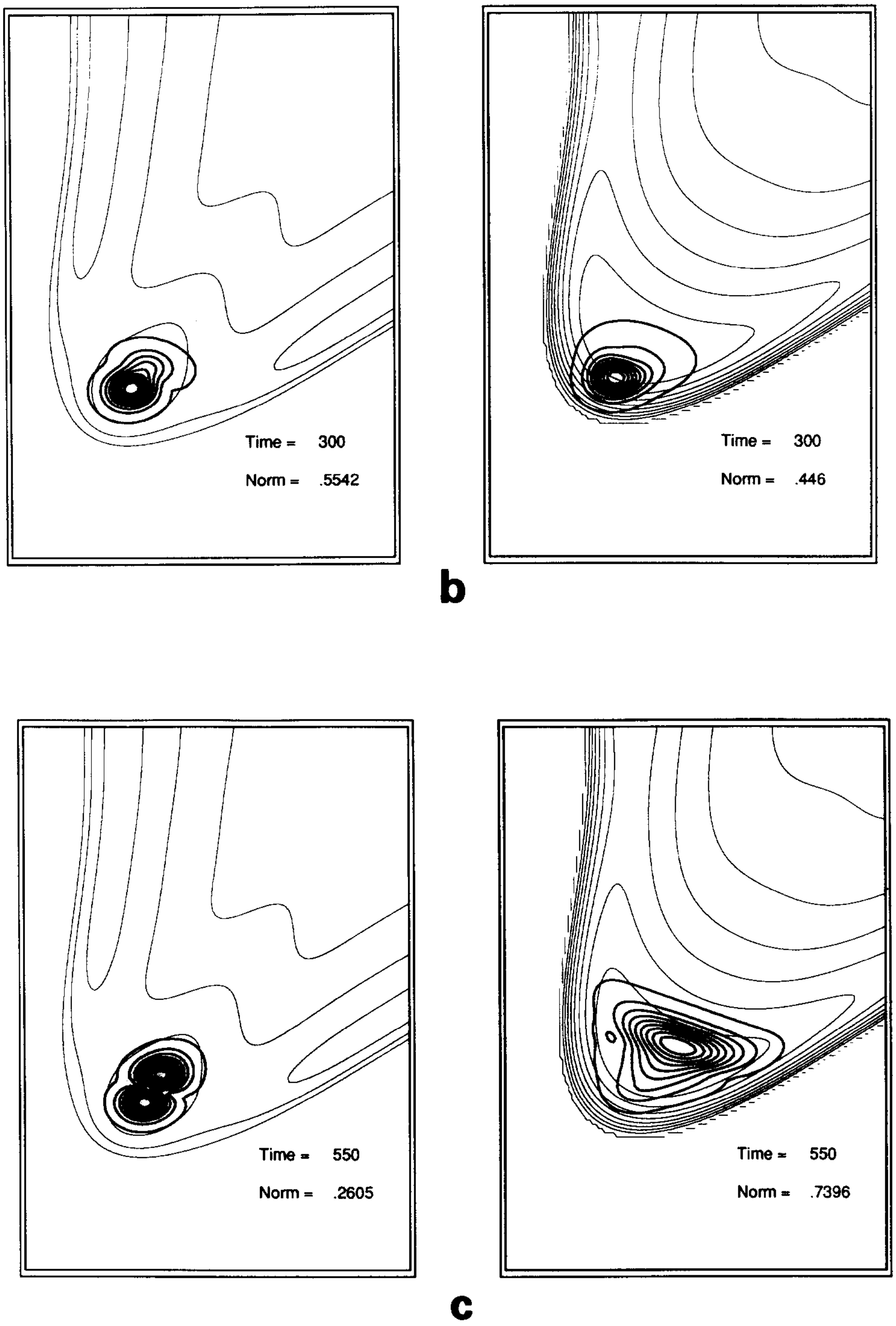

Fig. 2. (Continued on next page.)

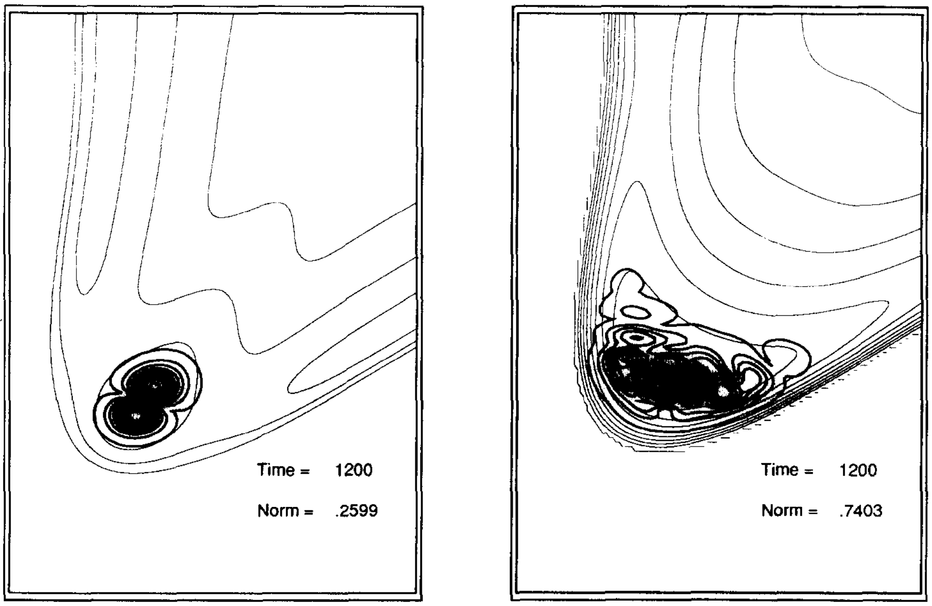
Time = 1200
Norm = .2599
Time = 1200
Norm = .7403

d

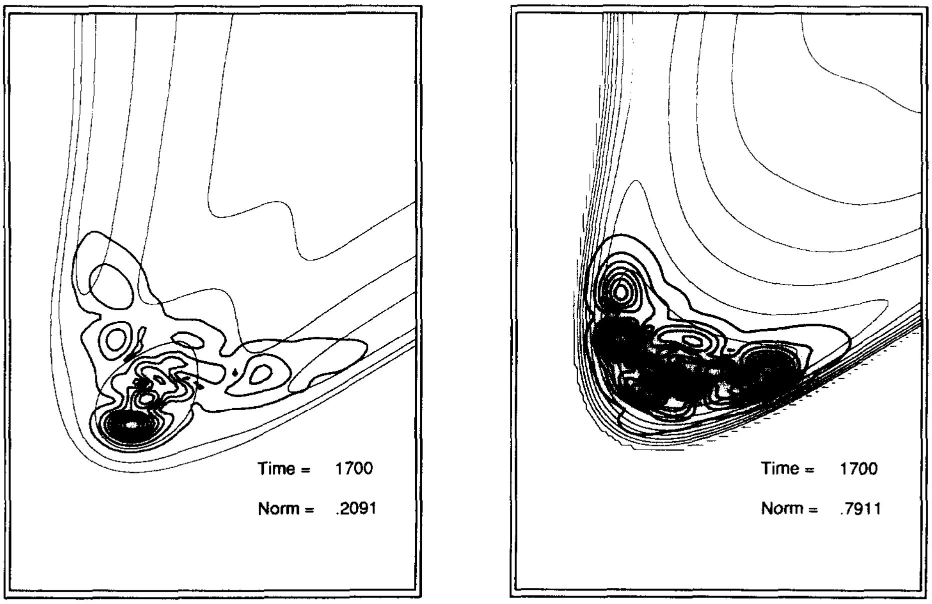
Time = 1700
Norm = .2091
Time = 1700
Norm = .7911

e

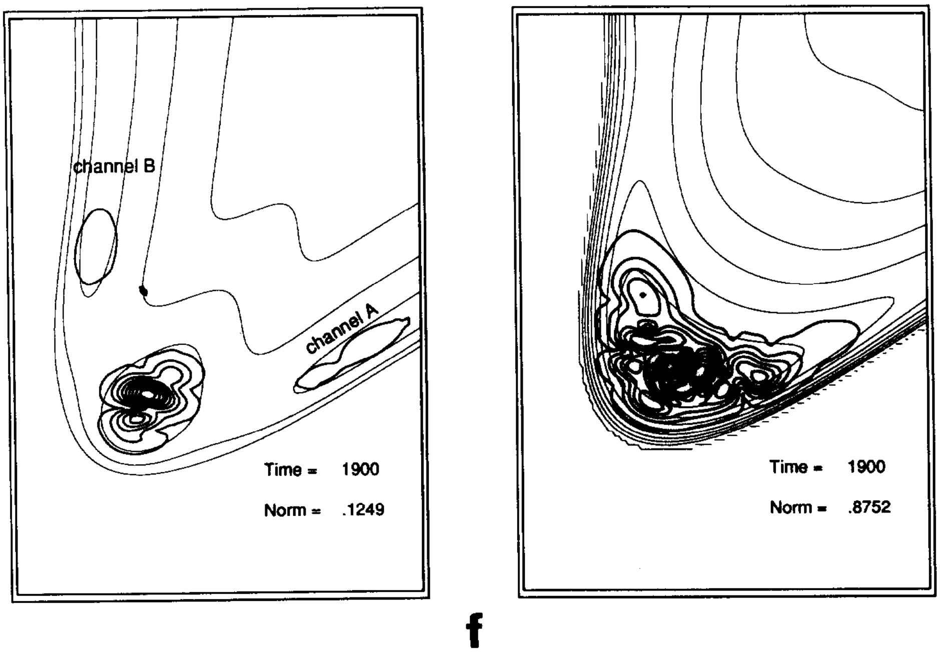

Fig. 2. The absolute square of the wavefunction on the ground and excited state surfaces superimposed on the potential energy surfaces. The snapshots were taken during the evolution of the wavefunction for the case of Gaussian pump and dump pulses; the pulse parameters are listed in table 1. (a) The wavefunction before the pump pulse is applied. Note that all the amplitude is on the ground state surface. The mesh used for these calculations was 64×64. (b) The wavefunction during the period in which the pump pulse acts. Note that the amplitude on the excited state is located on the repulsive wall of the potential energy surface and that the amplitude on the ground state surface corresponds to a vibrationally excited state. (c) The wavefunction after completion of the pump pulse. In this case, 74% of the amplitude has been transfered from the ground to the excited state surface. The remaining amplitude on the ground state surface is almost exclusively in the first excited state of the symmetric stretching mode. (d) The wavefunction just before the dump pulse. The "blender" effect of the large anharmonicity of the excited state potential energy surface is evident. (e) The wavefunction during the period in which the dump pulse acts. Note that the amplitude which is transferred from the excited to the ground state surface leads to reaction in both channels A and B. (f) The wavefunction after completion of the dump pulse, showing the amplitudes in reactive channels A and B (channel A = AA + B, channel B = A + AB). Note that the amplitudes in the two channels are approximately equal in magnitude, as expected given the strong defocussing characteristics of the shape of the excited state potential energy surface.

is at some intermediate time on the excited state surface.

The intuitive optimization method involves an iteration scheme and, therefore, requires an initial guess for the function to be optimized. The following form for the electromagnetic field pulse was used:

$$\mathcal{E}(t) = A_0 \exp[-(t-t_0)^2/2\sigma_0^2]\cos(\omega_0 t) + A_1 \exp[-(t-t_1)^2/2\sigma_1^2]\cos(\omega_1 t)\,, \tag{2.2}$$

where t_i is the time of pulse i ($i=0,1$) and, therefore, t_1-t_0 is the time delay between pulses. The other characteristic features of the pulse waveform are its central frequency ω_i, width σ_i and amplitude A_i. The form (2.2), with two Gaussian pulses with an adjustable time delay between them, was shown in our earlier study to give considerable control over the branching to different products. In principle, the pulse parameters and the time delay should be optimized for a particular channel before the iteration procedure is started; in practice, any reasonable set of initial values is acceptable. Fig. 2 displays the results of a calculation using (2.2) for the initial guess. Amplitude is transfered from the ground to the excited state surface by the first pulse and then back to the ground state surface by the second pulse. It is important to notice that wavefunction amplitude appears in

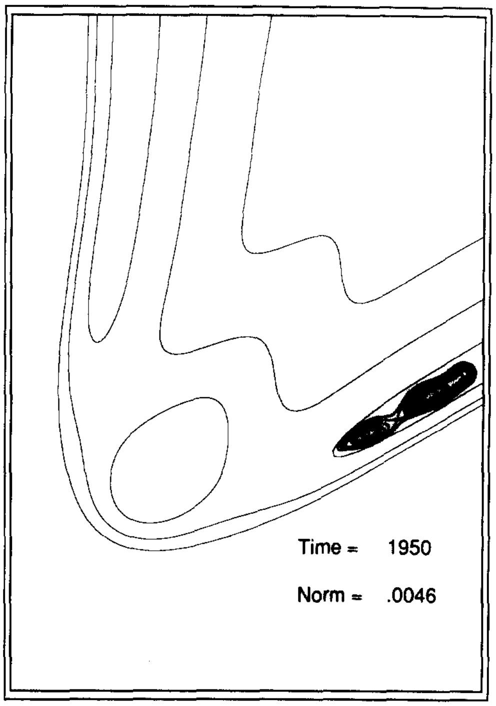

Fig. 3. The result of the action on the wavefunction of the projection operator selecting channel A.

both exit channels without apparent bias towards one or the other.

Consider, now, the wavefunction amplitude located in channel A, shown in fig. 3. The electromagnetic field waveform $\mathscr{E}(t)$ responsible for the creation of this amplitude is now sought. The inversion scheme is based on using eq. (2.1) to propagate the wavefunction amplitude backwards in time. Simultaneously, the wavefunction amplitude on the upper state surface is also propagated backwards in time. We must now affect the transfer of amplitude from ψ_g^{out} to the upper surface. We do this by choosing a field waveform 90° out of phase with the overlap between the wavefunctions on the two surfaces, i.e.

$$\mathscr{E}(t)=\mathrm{i}\langle\psi_g(t)|\mu_{ug}|\psi_u(t)\rangle C(t)\,, \tag{2.3}$$

where $C(t)$ is a positive function. The validity of (2.3) will be made apparent later, when the analysis of the global optimization scheme is presented. Inserting (2.3) into (2.1) we obtain

$$\partial\psi_g/\partial t=-\mathrm{i}\mathbf{H}_g\psi_g+C(t)\langle\psi_g|\mu_{ug}|\psi_u\rangle\mu_{ug}\psi_u\,, \tag{2.4}$$

which leads to a loss of amplitude from the ground state surface when propagating backwards in time since

$$\mathrm{d}\langle\psi_g|\psi_g\rangle/\mathrm{d}t=2C(t)|\langle\psi_g|\mu_{ug}|\psi_u\rangle|^2\,. \tag{2.5}$$

By virtue of microscopic reversibility this prescription for the choice of pulse leads to a gain of amplitude on the ground state surface when the propagation is in the forward direction in time. According to eqs. (2.3)–(2.5), wavefunction amplitude is transfered between the two surfaces with minimum power when the field is taken to be proportional to the overlap between the wavefunctions on the two surfaces. $C(t)$ may be then be taken to be a slowly varying envelope function.

The recipe for the local optimization procedure is now complete. Propagating in the positive direction of time, the first pulse transfers wavefunction amplitude from the ground state to the excited state surface. A π pulse, which can transfer all the amplitude from the lower to the upper surface is the most desirable, but any pulse that transfers a significant fraction of the amplitude is satisfactory. Now the second pulse, shaped to conform to the calculated $\mathscr{E}(t)$, is applied to the system. Consider a particular chemical outcome, defined by the wavefunction amplitude on the ground state surface at $t=t_f$, namely $\chi_g(t_f)$. This wavefunction is propagated backwards in time until all of its amplitude is transferred to the upper state surface, while $\mathscr{E}(t)$ is stored. If all of the ground state amplitude is transfered in the first backward propagation pass microscopic reversibility ensures that there is product selectivity in the forward propagation mode. It is more likely, however, that in the first backwards propagation pass only a fraction of the wavefunction amplitude is transferred from the ground to the excited state surface. In this case an iterative procedure is adopted to optimize the selectivity. First the calculated pulse shape $\mathscr{E}(t)$ is used to propagate the wavefunction amplitude forward in time and the desired product is selected by application of the appropriate projection operator (i.e. $|\chi_g(t_f)\rangle\langle\chi_g(t_f)|$, where $\chi_g(t_f)$ is the target state). Then a backwards propagation is started to calculate a new pulse shape $\mathscr{E}'(t)$. The iterative process is stopped when the product selectivity, e.g., the ratio of numbers of product molecules formed, achieves a predetermined value, or a fixed point is reached which determines, at least locally, the maximum selectivity possible.

2.2.2. Global optimization of product selectivity

In this section we use optimal control theory to provide a rigorous procedure for the determination of the electromagnetic field pulse shape that maximizes the selectivity of a particular reaction product. It will be seen that all the key features in the intuitive approach described above emerge in a natural fashion from the formalism of optimal control theory.

Consider, first, the objective, or target, functional

$$J=\langle\psi(t_f)|\mathbf{P}|\psi(t_f)\rangle\,, \tag{2.6}$$

where $\mathbf{P}$ is a projection operator which selects the desired exit channel, in our case the part of the wavefunction which is beyond the saddlepoint on the groundstate surface and which is characterized by outgoing momentum (with respect to the exit channel). We wish to optimize the target function. Note that t_f is the final time, after the pulse sequence has been shut off, and we assume the limit $t_f\to\infty$ exists.

A constraint involving the total energy in the field must be imposed on the optimization procedure. This constraint takes the form

$$\int_{t_0}^{t_f} \mathrm{d}t\, \mathscr{E}(t)\mathscr{E}^*(t) = \int_{t_0}^{t_f} \mathrm{d}t\, [\mathrm{Re}\, \mathscr{E}^2(t) + \mathrm{Im}\, \mathscr{E}^2(t)] = E\,, \tag{2.7}$$

where E is the energy of the pulse. The maximization of J, subject to the constraints arising from the equation of motion of ψ and the total energy in the light field, can be converted into an unconstrained optimization by using Lagrange multipliers χ and λ,

$$\bar{J}=\langle\psi(t_f)|\mathbf{P}|\psi(t_f)\rangle + \mathrm{i}\int_{t_0}^{t_f} \mathrm{d}t\, (\langle\chi|\mathrm{i}\,\partial/\partial t-\mathbf{H}|\psi\rangle+\mathrm{c.c.}) + \lambda\left(\int_{t_0}^{t_f} \mathrm{d}t\, [\mathrm{Re}\, \mathscr{E}^2(t)+\mathrm{Im}\, \mathscr{E}^2(t)] - E\right). \tag{2.8}$$

In (2.8), ψ is a two-vector and $\mathbf{H}$ is a 2×2 matrix (see eq. (2.1)). The variation of $\bar{J}$ is taken with respect to $\mathscr{E}$ and ψ: $\delta\bar{J}=0$ for $\delta\,\mathrm{Re}\,\mathscr{E}$, $\delta\,\mathrm{Im}\,\mathscr{E}$ and $\delta\psi$. We find

$$\begin{aligned}
\delta\bar{J} = {} & \langle \delta\psi(t_\mathrm{f}) | \mathbf{P} | \psi(t_\mathrm{f}) \rangle + \langle \psi(t_\mathrm{f}) | \mathbf{P} | \delta\psi(t_\mathrm{f}) \rangle + \int_{t_0}^{t_\mathrm{f}} \mathrm{d}t\, (\mathrm{i}\langle \delta\psi | \mathbf{H} | \chi \rangle - \mathrm{i}\langle \chi | \mathbf{H} | \delta\psi \rangle - \langle \delta\dot{\psi} | \chi \rangle - \langle \chi | \delta\dot{\psi} \rangle) \\
& + \int_{t_0}^{t_\mathrm{f}} \mathrm{d}t\, \delta\,\mathrm{Re}\,\mathscr{E}\, (2\lambda\,\mathrm{Re}\,\mathscr{E} + \mathrm{i}\langle \psi | \partial\mathbf{H}/\partial\,\mathrm{Re}\,\mathscr{E} | \chi \rangle - \mathrm{i}\langle \chi | \partial\mathbf{H}/\partial\,\mathrm{Re}\,\mathscr{E} | \psi \rangle) \\
& + \int_{t_0}^{t_\mathrm{f}} \mathrm{d}t\, \delta\,\mathrm{Im}\,\mathscr{E}\, (2\lambda\,\mathrm{Im}\,\mathscr{E} + \mathrm{i}\langle \psi | \partial\mathbf{H}/\partial\,\mathrm{Im}\,\mathscr{E} | \chi \rangle - \mathrm{i}\langle \chi | \partial\mathbf{H}/\partial\,\mathrm{Im}\,\mathscr{E} | \psi \rangle)\,. \qquad (2.9)
\end{aligned}$$

Integrating (2.9) by parts leads to

$$\begin{aligned}
\delta\bar{J} = {} & \langle \delta\psi(t_0) | \chi(t_0) \rangle + \langle \chi(t_0) | \delta\psi(t_0) \rangle + \langle \delta\psi(t_\mathrm{f}) | \mathbf{P} | \psi(t_\mathrm{f}) \rangle \\
& - \langle \delta\psi(t_\mathrm{f}) | \chi(t_\mathrm{f}) \rangle - \langle \chi(t_\mathrm{f}) | \delta\psi(t_\mathrm{f}) \rangle + \langle \psi(t_\mathrm{f}) | \mathbf{P} | \delta\psi(t_\mathrm{f}) \rangle \\
& + \int_{t_0}^{t_\mathrm{f}} \mathrm{d}t\, (\mathrm{i}\langle \delta\psi | \mathbf{H} | \chi \rangle - \mathrm{i}\langle \chi | \mathbf{H} | \delta\psi \rangle + \langle \delta\psi | \dot{\chi} \rangle + \langle \dot{\chi} | \delta\psi \rangle) \\
& + \int_{t_0}^{t_\mathrm{f}} \mathrm{d}t\, \delta\,\mathrm{Re}\,\mathscr{E}\, (2\lambda\,\mathrm{Re}\,\mathscr{E} + \mathrm{i}\langle \psi | \partial\mathbf{H}/\partial\,\mathrm{Re}\,\mathscr{E} | \chi \rangle - \mathrm{i}\langle \chi | \partial\mathbf{H}/\partial\,\mathrm{Re}\,\mathscr{E} | \psi \rangle) \\
& + \int_{t_0}^{t_\mathrm{f}} \mathrm{d}t\, \delta\,\mathrm{Im}\,\mathscr{E}\, (2\lambda\,\mathrm{Im}\,\mathscr{E} + \mathrm{i}\langle \psi | \partial\mathbf{H}/\partial\,\mathrm{Im}\,\mathscr{E} | \chi \rangle - \mathrm{i}\langle \chi | \partial\mathbf{H}/\partial\,\mathrm{Im}\,\mathscr{E} | \psi \rangle)\,. \qquad (2.10)
\end{aligned}$$

The functional form of the initial wavepacket is not subject to variation, so the first two terms in (2.10) vanish. From the variational equation we obtain the equation of motion for the Lagrange multiplier χ,

$$\mathrm{i}\partial\chi/\partial t = \mathbf{H}\chi\,, \qquad (2.11)$$

which is just the time dependent Schrödinger equation subject to the final condition

$$|\chi(t_\mathrm{f})\rangle = \mathbf{P} | \psi(t_\mathrm{f}) \rangle\,, \qquad (2.12)$$

which relates χ to ψ on the boundary. The pulse shape is then given, except for normalization, by

$$\mathscr{E}(t) = (\mathrm{i}/2\lambda)\,[\langle \chi(t) | \partial\mathbf{H}/\partial\,\mathrm{Re}\,\mathscr{E} + \mathrm{i}\partial\mathbf{H}/\partial\,\mathrm{Im}\,\mathscr{E} | \psi(t) \rangle - \mathrm{i}\langle \psi(t) | \partial\mathbf{H}/\partial\,\mathrm{Re}\,\mathscr{E} + \mathrm{i}\partial\mathbf{H}/\partial\,\mathrm{Im}\,\mathscr{E} | \chi(t) \rangle]\,. \qquad (2.13)$$

Because of the matrix form of the Hamiltonian (2.1) the derivatives in (2.13) take the form

$$\partial\mathbf{H}/\partial\,\mathrm{Re}\,\mathscr{E} + \mathrm{i}\partial\mathbf{H}/\partial\,\mathrm{Im}\,\mathscr{E} = \mu \begin{pmatrix} 0 & 2 \\ 0 & 0 \end{pmatrix}. \qquad (2.14)$$

Finally, the electromagnetic field pulse shape is related to the overlap function $O(t)$ by

$$\mathscr{E}(t) = \frac{\mathrm{i}}{\lambda}\,[\langle \chi_\mathrm{u}(t) | \mu_\mathrm{ug} | \psi_\mathrm{g}(t) \rangle - \langle \psi_\mathrm{u}(t) | \mu_\mathrm{ug} | \chi_\mathrm{g}(t) \rangle] \equiv \lambda^{-1} O(t)\,. \qquad (2.15)$$

Note the similarity between eqs. (2.15) and (2.3); the optimal pulse is found to be 90° out of phase with the wavefunction overlap. The normalizing factor, i.e. the real Lagrange multiplier λ, is then evaluated from the constant energy constraint,

$$\lambda^{-2}\int_{t_0}^{t_f} \mathrm{d}t\, |O(t)|^2 = E\,, \tag{2.16}$$

so that

$$\lambda = \pm\left(\frac{1}{E}\int_{t_0}^{t_f} \mathrm{d}t\, |O(t)|^2\right)^{1/2}\,. \tag{2.17}$$

3. Numerical calculations and results

The iteration procedure we have used to determine the optimal pulse shape for enhancing production of a particular product of a reaction is as follows:

(a) Assume a form for the initial pulse shape $\mathscr{E}(t)$.

(b) Integrate the Schrödinger equation

$$\mathrm{i}\partial\psi/\partial t = \mathbf{H}(t)\psi(t) \tag{2.18}$$

forward to time t_f, starting from the initial condition in which the wavefunction amplitude is entirely in the ground state of the lower electronic surface.

(c) Apply the projection operator that selects the exit channel to $\psi(t_f)$ and obtain the value of $\chi(t_f)$, regarded as an initial value for the backward propagation.

(d) Propagate χ backwards in time using the Schrödinger equation

$$\mathrm{i}\partial\chi/\partial t = \mathbf{H}(t)\chi(t)\,. \tag{2.19}$$

Propagate the original wavefunction ψ backwards as well, in parallel (this last step to eliminate storage).

(e) During this propagation calculate the overlap function

$$O(t) = \mathrm{i}[\langle\chi_u(t)|\mu_{ug}|\psi_g(t)\rangle - \langle\psi_u(t)|\mu_{ug}|\chi_g(t)\rangle]\,. \tag{2.20}$$

(f) When the backward propagation is complete renormalize the result to obtain the new electromagnetic field pulse waveform

$$\mathscr{E}(t) = O(t)\left(\frac{1}{E}\int_{t_0}^{t_f} \mathrm{d}t\, |O(t)|^2\right)^{-1/2}\,. \tag{2.21}$$

(g) Restart at step (b) with the result of step (f) for the waveform.

(h) Terminate the iterative procedure when convergence has been achieved.

Before proceding further it is worthwhile noting that one of the obstacles to obtaining insight concerning the selectivity process is the proper interpretation of the time energy uncertainty relation inherent in the pulse shape $\mathscr{E}(t)$. We have found that a time–frequency phase space representation allows a clear description of the pulse shape. We have chosen to use the Wigner distribution function [10] for this representation:

$$W(t,\omega) = \frac{1}{\pi}\int_{t_0}^{t_f} \mathrm{d}s[\mathscr{E}(t+s)\mathscr{E}^*(t-s)]\exp(2\mathrm{i}\omega s)\,. \tag{2.22}$$

A frequency based selectivity process is a horizontal density profile of the Wigner distribution function, while a vertical density profile corresponds to a time delay type selectivity process. The procedure described in this paper seeks windows in the time–energy phase space which optimize formation of a specific product of a reaction.

Both the local and global optimization methods described rely heavily on an efficient, accurate and stable solver of the time dependent Schrödinger equation. The method we have used is a two surface modification of the Fourier transform method [11,12] used to calculate the Hamiltonian operation $\phi = \mathrm{H}\psi$. The initial wavefunction was chosen to be that for the ground vibrational state of the lower potential energy surface. This state was produced by propagating a trial wavefunction in imaginary time [13] until only the ground state amplitude survives. The time propagation was carried out with a second-order differencing scheme with a small time step (0.5 au). To check the convergence of the calculations the time step was varied over a factor of four and the mesh in the Fourier transform procedure over a factor of two. In the case of the global optimization scheme, the iterative procedure caused severe feedback type instabilities when more than four iterations were attempted. Therefore, for some of the calculations the propagator was replaced by a fifth-order polynomial approximation to the evolution operator [14].

4. Results

The model we have chosen for demonstration of the principles of optimal control of selectivity of product formation is, in a sense, a very difficult case for several reasons. First, the two chemical channels differ only by their mass combination so that the products are only isotopically different. Second, the excited state potential energy surface has been constructed with extremely large anharmonic terms, which generate a "blender" effect on the wavefunction. The chemical selectivity is defined by two projection operators which select the wavefunction beyond the saddlepoints of the ground state potential energy surface, leading to channel A or channel B. Fig. 3 displays the operations of the projection operators on a typical wavefunction. Before applying our scheme to control the selectivity of product formation a control calculation was carried out. Specifically, a series of pump and dump pulses with different time delays and different shapes were applied to the model system for the purpose of determining the inherent bias in product formation. The results show a small preference for channel A by ratio of 5 : 4 to 3 : 2. These results confirm the prediction that the excited state potential surface chosen has a strong scrambling effect because of the extensive spatial delocalization on the excited state surface. The total yield of products was found to be low, varying from 10^{-4} to 10^{-2}.

The local optimization scheme was at first applied to the second (dump) pulse only, and then later for some cases to both pump and dump pulses. The procedure was used to optimize the yield in channel A. After selecting the product channel the iteration scheme was started. The normalization of the product channel was adjusted, arbitrarily, to 26.6%. The backward propagation continued until the initial time was reached. A positive envelope function (eq. (2.5)) was invoked to limit the pulse duration; its functional form was a sum of Gaussians. Then, using the calculated waveform, forward propagation was carried out to the final time, selecting channel A, and the procedure repeated. After a few rounds (typically, three) a fixed point was reached, corresponding to a selectivity ratio of 5 : 2 in favor of channel A, with a total yield of 16%. Fig. 4a displays the Wigner distribution of the pulse that produced this result. Fig. 5a displays the pulse as a function of time. Fig. 6 displays the evolution of the wavefunction under this pulse. Repeating the procedure with respect to optimizing the yield in channel B, a selectivity ratio of 7 : 8 was obtained with a total yield of 8%. Fig. 4b displays the Wigner distribution optimized for channel B, while fig. 4c compares the pulse that enhances the yield in channel A to the pulse that enhances the yield in channel B. Optimizing the pump pulse as well as the dump pulse improved the selectivity of the yield in channel B to 2 : 3.

The global optimal control procedure was carried out with a grid of 64×64 for a total time of 2000 au. The shorter time period over which the optimization was carried out, relative to that used in the local optimization procedure, restricts the adaptation of the pulse to the surfaces and the applied field, hence in principle also restricts the extent of optimization to less than that attainable with longer propagation time. In turn this implies that our calculation of the globally optimal pulse shape can have less selectivity than one optimized over a longer period. We note that the optimization procedure was constructed to produce high yields with a limited amount of energy per pulse. The control function optimized was the difference between the yields in the two channels.

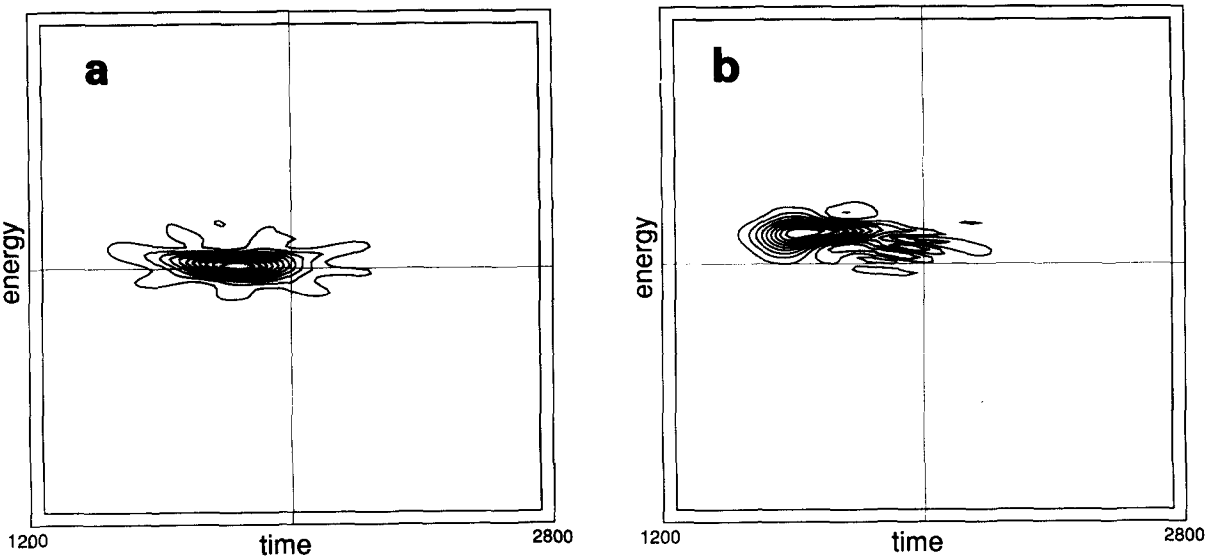

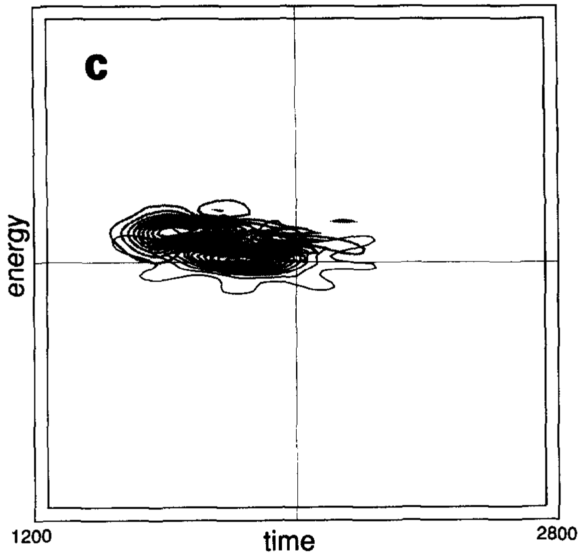

Fig. 4. (a) The Wigner distribution function of the pulse which leads to optimal yield of product in channel A as calculated using the local optimization procedure. (b) The Wigner distribution function of the pulse which leads to optimal yield of product in channel B as calculated using the local optimization procedure. (c) A comparison of the Wigner distributions of the pulses that optimize the yields in channels A and B. Note that these pulses have different peaks in time and in energy.

Fig. 7 displays the Wigner distribution function of an optimal pulse and fig. 8 displays the wavefunction under the influence of this pulse. For the case of optimization of the yield in channel A we find a selectivity ratio of 13 : 3, with an overall yield of 13.2%. We note that the optimized pulse is chirped, i.e. does not have a simple shape.

It should be pointed out that the results reported in this paper are based on iterative calculations which use a simple numerical criterion for convergence of the calculations. While this appears completely satisfactory for the local optimization scheme, the global optimization scheme is more demanding and the calculations correspondingly more tedious. We believe the results presented are correct, but also are developing an improved computational scheme which embodies elements of both conjugate gradient and iterative procedure [15].

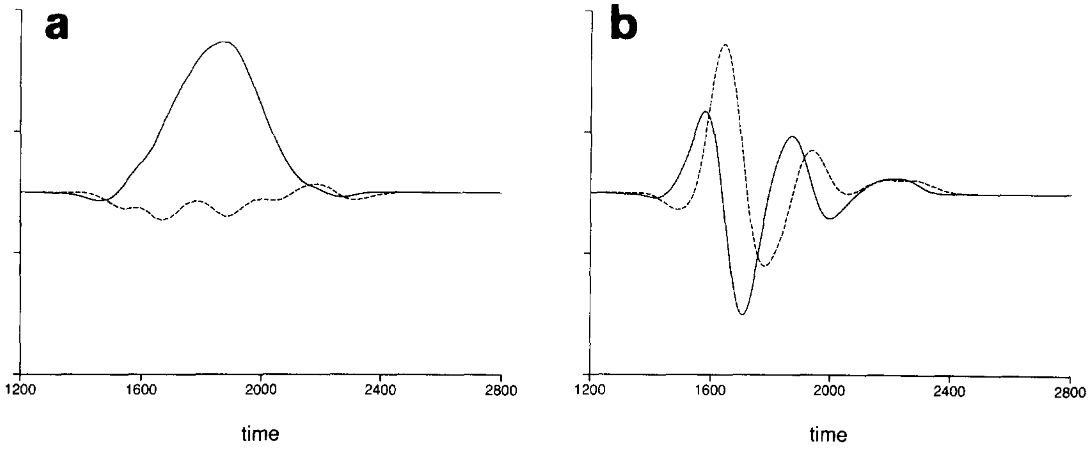

Fig. 5. (a) The electromagnetic field pulse for optimal yield in channel A, as a function of time. The solid line is the real part of the function, the dashed line the imaginary part of the function. (b) The electromagnetic field pulse for optimal yield in channel B, as a function of time. The solid and dashed lines have the same meaning as in (a).

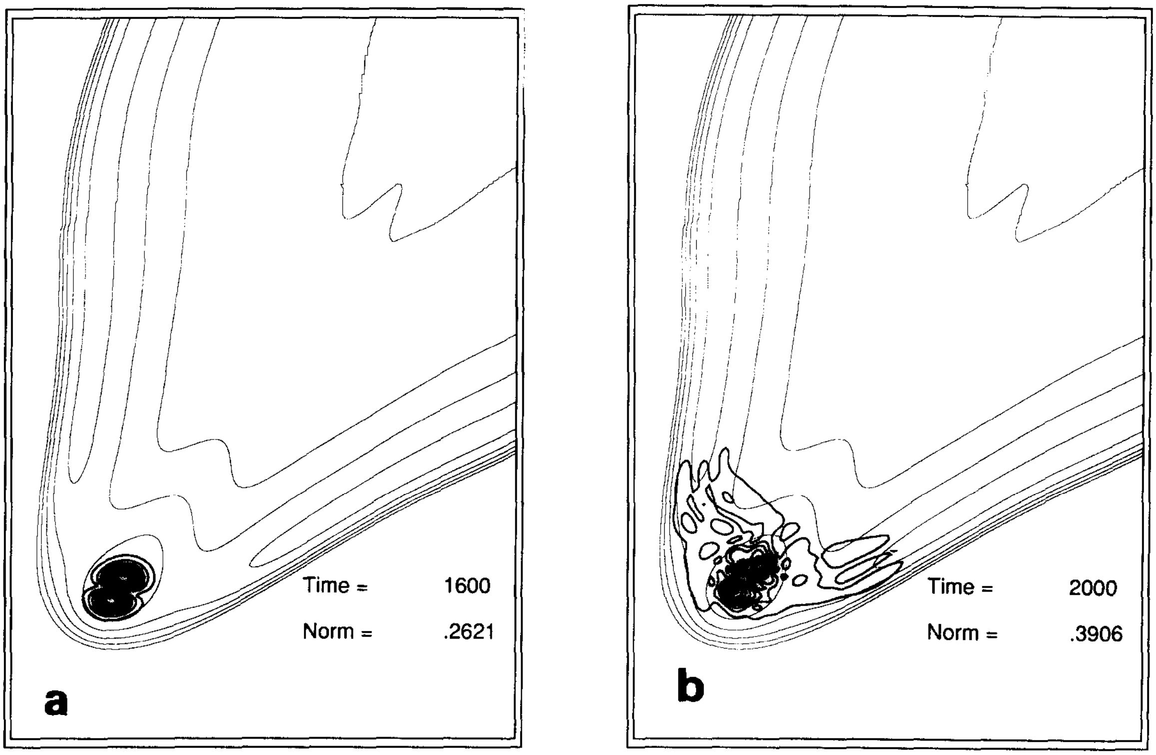

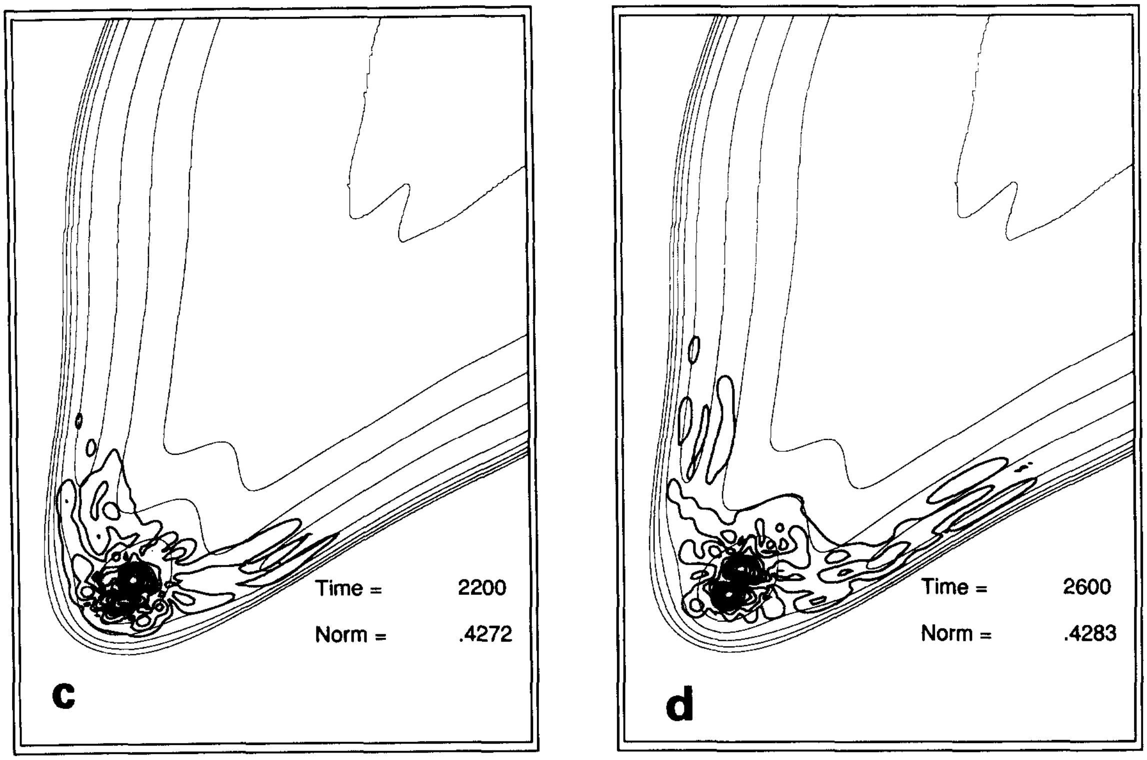

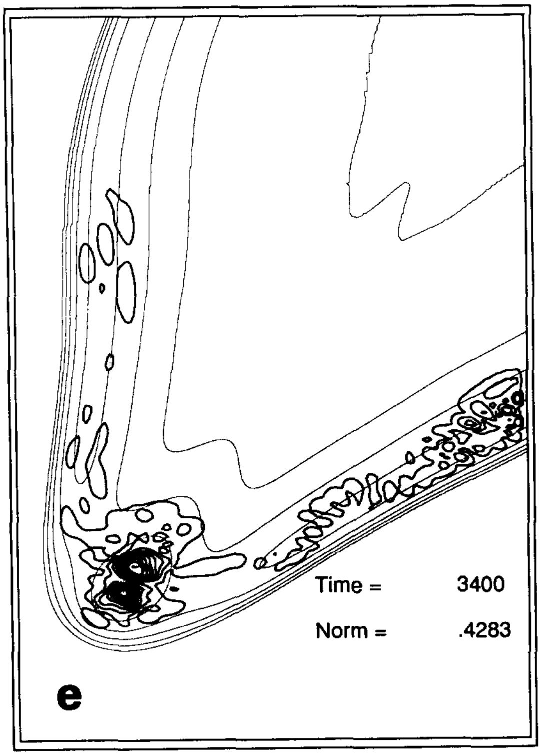

Fig. 6. The evolution of the wavefunction under the influence of the pulse shown in fig. 5a. The mesh used for these calculations was 96×96.

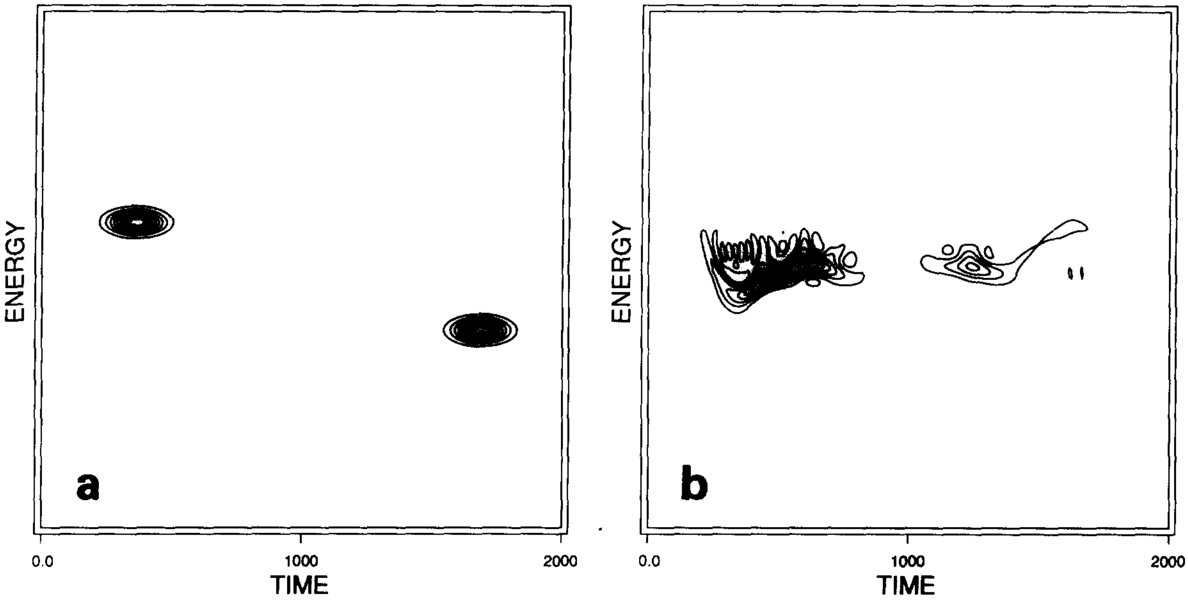

Fig. 7. (a) The Wigner distribution function corresponding to the initial guess waveform for the global optimization of the yield in channel A. (b) The Wigner distribution function which leads to optimal yield of product in channel A as calculated using the global optimization procedure.

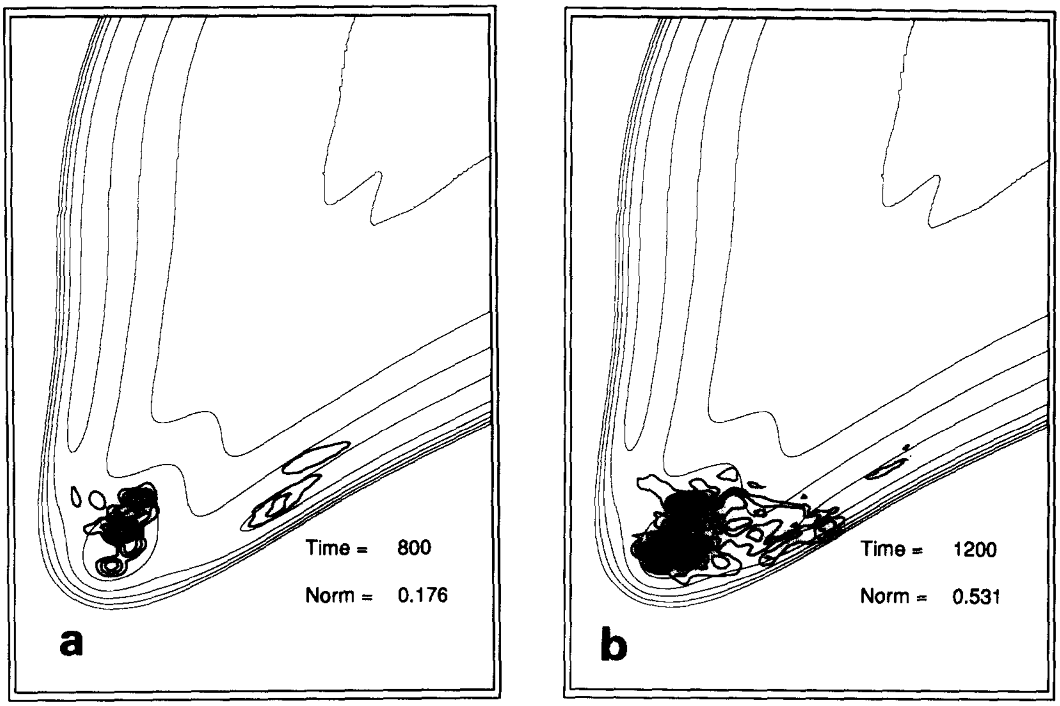

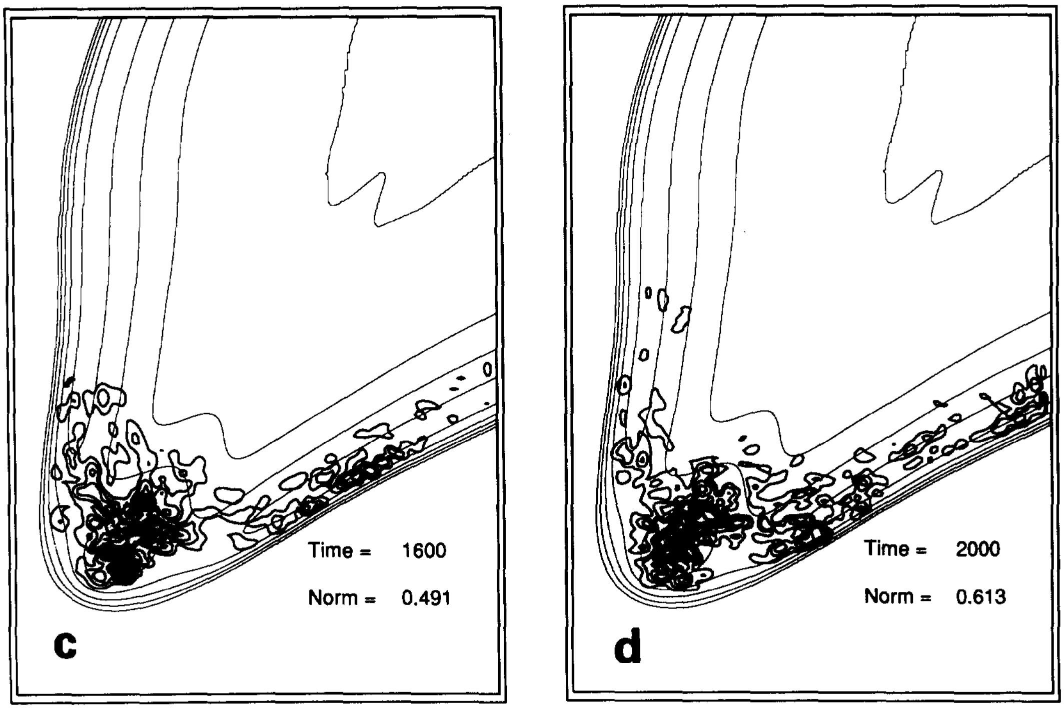

Fig. 8. The evolution of the wavefunction under the influence of the pulse shown in fig. 7b.

5. Discussion

This paper describes a new theoretical algorithm for optimizing the selectivity of product formation in a chemical reaction, within the framework of the Tannor–Rice pump–dump selectivity scheme. The selectivity procedure described is, basically, a search for a window (or windows) in time–energy phase space wherein the coherence inherent in the wavefunction naturally leads to an optimal differentiation between the yields of different products. It should be noted that the procedure described in this paper goes far beyond the optimization procedure described in the original publication by Tannor and Rice [4]. Whereas that optimization was based on a perturbation theory weak field analysis of the system, the new procedure accounts for the interaction of the reactive system with strong fields. Indeed, the fields considered are so strong that, when on, the states of the system are strongly mixed field–matter combinations. In this regime, the application of the external field to the reactive system strongly alters the dynamics of the reactive system. The simplest application of the selectivity procedure requires interaction of the reactive system with varying delay times and central frequencies. We have shown that pulse shaping can be used to alter the product selectivity even in a worst case situation where the product species are slightly different isotopomers. We expect, as we learn how to treat the optimization problem more accurately, and as we consider the advantages conferred by use of multiple pulse sequences, that control of selectivity of product formation will improve from the level demonstrated in this paper.

Acknowledgement

The portion of this work carried out at the Hebrew University was partially supported by Convex of Israel

Inc. and by a grant to the Fritz Haber Institute from the Minerva Gesellschaft für GmbH, Munich, FRG. The portion of this work carried out at The University of Chicago was supported by a grant from the National Science Foundation. The portion of this work carried out at the Illinois Institute of Technology was supported by grants from the National Science Foundation and the Research Corporation. DJT is grateful to Dr. Michael J. Davis of the Argonne National Laboratory for a very useful comment concerning the utility of the Wigner function representation introduced in section 3. PG is Charge de Recherches of the Belgian National Fund for Scientific Research.

References

[1] N.J. Turro, Molecular Photochemistry (Benjamin, New York, 1967).
[2] J. Jortner, R.D. Levine and S.A. Rice, eds., Advances in Chemical Physics, Vol. 47. Photoselective Chemistry (Wiley, New York, 1981).
[3] A. Carrington and R.A. Kennedy, J. Chem. Phys. 81 (1984) 9;
A. Carrington and I.R. McNaib, Accounts Chem. Res. 22 (1989) 218.
[4] B. Hartke, J. Manz and J. Mathis, Chem. Phys. 139 (1989) 123.
[5] P. Brumer and M. Shapiro, Chem. Phys. Letters 126 (1986) 54;
M. Shapiro and P. Brumer, J. Chem. Phys. 84 (1986) 4103.
[6] D.J. Tannor and S.A. Rice, J. Chem. Phys. 83 (1985) 5013.
[7] D.J. Tannor, R. Kosloff and S.A. Rice, J. Chem. Phys. 85 (1986) 5805.
[8] S.A. Rice, D.J. Tannor and R. Kosloff, J. Chem. Soc. Faraday Trans. II 82 (1986) 2423.
[9] A.P. Peirce, M.A. Dahleh and H. Rabitz, Phys. Rev. A 37 (1989) 4950;
S. Shi, A. Woody and H. Rabitz, J. Chem. Phys. 88 (1988) 6870.
[10] E.P. Wigner, Phys. Rev. 40 (1932) 749;
M. Hillery, R.F. O'Connell, M.O. Sculley and E.P. Wigner, Phys. Rept. 106 (1984) 193.
[11] D. Kosloff and R. Kosloff, J. Comput. Phys. 52 (1983) 35.
[12] R. Kosloff and D. Kosloff, J. Chem. Phys. 79 (1983) 1823.
[13] R. Kosloff and H. Tal-Ezer, Chem. Phys. Letters 127 (1986) 223.
[14] R. Kosloff, H. Tal-Ezer and C. Cerjan, J. Comput. Phys., submitted.
[15] S. Tersigni, P. Gaspard, S.A. Rice, R. Kosloff and D.J. Tannor, work in progress.